

## Semiconductor Interface Structure Studied by X-Ray Diffraction

Koichi Akimoto

*Department of Quantum Engineering, Nagoya University, Furo-cho, Chikusa-ku, Nagoya 464-01, Japan*

(Received January 21, 1997)

Semiconductor interface structures have been studied by employing the technique of grazing incidence X-ray diffraction (GID) with the use of synchrotron radiation.

Multiple-wavelength anomalous dispersion (MAD) method, a powerful direct method, has been modified and applied for the first time to an interface. This allows us to separate heavy and light atoms in a model-independent fashion and so deduce the structure. Of the numerous  $\sqrt{3}$  structures, only boron induced  $\sqrt{3}$  structure has been observed in the buried interface. MAD method has been applied to the Si/B $\sqrt{3}$ /GeSi(111) interface structure and direct evidence for ordering of the Ge and Si atoms at this interface has been obtained. Specially, it has been found that boron lies in a substitutional site surrounded by four nearest-neighbor Si atoms with Ge in the other sites.

In order to study the stress at the SiO<sub>2</sub>/Si interface, the X-ray intensity of the silicon substrate 311 reflection in an extremely asymmetric scheme of small incident angle and large exit angle has been measured for various silicon oxide thickness. X-ray rocking curve studies reveal that silicon substrate lattice is highly stressed even in the thin-SiO<sub>2</sub>/Si interface.

**KEYWORDS:** X-ray diffraction, interface, semiconductor

### 1. Introduction

Heterojunctions are widely used in semiconductor devices. In these systems, the interface often play an important role in the determination of physical characteristics. Although various kinds of techniques to study the structure of surfaces have been developed: scanning tunneling microscopy (STM), low energy electron diffraction (LEED), reflected high energy electron diffraction (RHEED), and X-ray diffraction, many of them are not effective enough to investigate interfaces because of their small penetration depth. Among them, X-ray diffraction is suited for interface studies due to the strong penetrating power. Due to this property, X-ray diffraction serves as a non-destructive method to investigate the buried interfaces and deformations of underlying layers caused by the surface structure. Moreover in-situ observations in liquid and gas environments as well as UHV condition can be performed to study the surfaces and interfaces.

X-ray diffraction was so far considered to be not suited for surface and interface studies due to low interaction of X-rays with a matter. However, recent developments of diffraction techniques together with synchrotron radiation sources have made it possible to study the structure of surfaces and interfaces. Moreover, extensive studies have revealed importance and superiority of X-ray diffraction. A great advantage of using X-ray diffraction is that scattering phenomena from surfaces and interfaces are interpreted by a single scattering theory in contrast to electron diffraction interpreted by a multiple scattering theory. This makes it quite easy to analyze the experimental data, and allows us to apply the analyzing methods well-developed for three-dimensional crystallography to the analysis of surfaces and interfaces.

We review our results on interface structures studied by employing the technique of grazing incidence X-ray diffraction (GID) with the use of synchrotron radiation.

### 2. Interface Superstructure

Of the numerous  $\sqrt{3}$  structures, only boron induced  $\sqrt{3}$  structure has been observed in the buried interface.<sup>1)</sup> Interface  $\sqrt{3}$  structure is expected to create a new class of so-called  $\delta$ -doped materials, in which holes produced by boron are trapped at the two-dimensional interface.

Unlike other group-III elements on the Si(111) surface, boron is found to substitute for one of the Si atoms, resulting in a very stable structure. However, because of the small size of boron, the four surrounding Si atoms must shift appreciably towards it. It is thought that including Ge in the system should partially relieve some of the strain, since Ge is larger than both Si and boron, resulting in an even more stable interface. In addition, band bending at the Si/B $\sqrt{3}$ /GeSi(111) interface due to the different band gaps of Si and GeSi should improve the hole-trapping properties. It is necessary to determine the structure of Si/B $\sqrt{3}$ /GeSi(111) and understand the reasons for its atomic arrangement.

This structure was derived by applying a direct method to anomalous X-ray diffraction data.<sup>2)</sup> This technique, known as multiple-wavelength anomalous dispersion (MAD) method,<sup>3)</sup> has been successfully used in protein crystallography for about ten years, and has been made appropriate modifications to facilitate its use in studying surfaces and interfaces. Anomalous dispersion effects themselves, have the ability of separating out heavier atoms.<sup>4)</sup>

The experiment consisted of using grazing incidence X-ray diffraction techniques to obtain the integrated intensities of ten  $\sqrt{3}$  reflections. Synchrotron radiation source of the Photon Factory of the National Laboratory for High Energy Physics (KEK) in Tsukuba, Japan was used.

Integrated intensities were measured as a function of X-ray energy across the Ge K-shell absorption edge, as in Fig. 1.

Most of the data looks like Fig. 1(a) which shows a

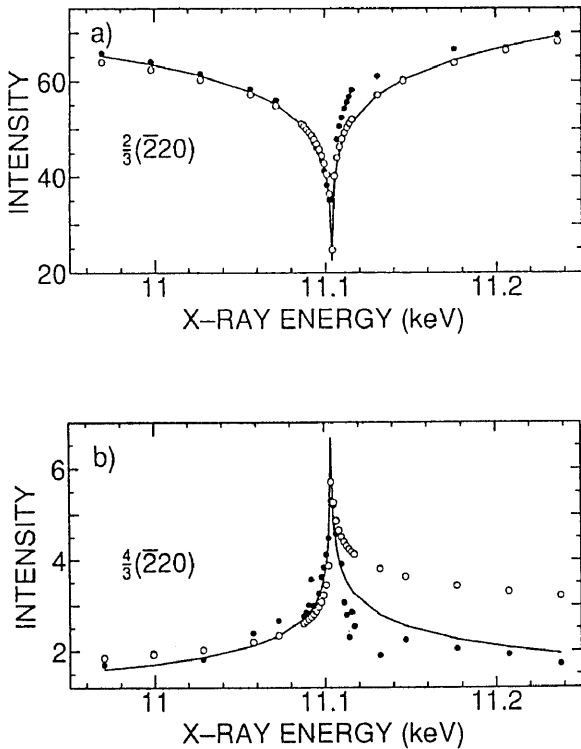


Figure 1. Intensity vs. energy for the reconstructed reflections (a)  $(hkl)=2/3 (\bar{2}20)$  and (b)  $(hkl)=4/3 (\bar{2}20)$ . The data (solid circles), the fit by the MAD analysis (line), and the fit with the model structure of Fig. 3 (open circles) are shown.

strong peak that decreases in intensity near the edge, but notice Fig. 1(b) shows a very weak reflection that increases in intensity. This sort of data lends itself very well to analysis by MAD. By separating out the anomalous part, the structure factor for the boron and Si atoms and the structure factor for the normal part of the Ge atoms are independently obtained through fitting to the data.<sup>5</sup> These fits are also shown in Fig. 1.

From the resulting set of fitted structure factors, separate partial Patterson maps for boron and Si, Fig. 2(a) and for Ge, Fig. 2(b) are generated. The maps are quite different, providing direct, model-independent evidence that the Ge and Si atoms occupy different sites (Fig. 2(a) should be dominated by Si). Interpreting the maps based on Fig. 2(c), it is apparent that sites A and B are Si while sites C and D are mostly Ge.

This interpretation leads to the model shown in Fig. 3 which was refined by fitting to the data of Fig. 1. It is found that the boron is in a Si substitutional site (site A, the center of the distortion in Fig. 2(c)) surrounded by four Si nearest-neighbor atoms, with the other sites dominated by Ge. Note that both the boron site and the distortion of the first layer Si are the same as in the  $B\sqrt{3}/Si(111)$  system.<sup>6</sup>

From the structure model, diffracted intensity was calculated as shown in Fig. 4, which is compared with measured one. Measurements of  $\sqrt{3}$  reflections were made at just two X-ray energies, at  $E=11.098\pm 0.002$  keV, near the Ge K-shell absorption edge (11.104 keV) (Fig. 4(b)), and at  $8.266\pm 0.002$  keV, far from the edge (Fig. 4(a)). In Fig. 4, the area of each circle is proportional to the observed intensity after correcting for polarization, Lorentz factor, and variation of the active sample area. The uncertainties were

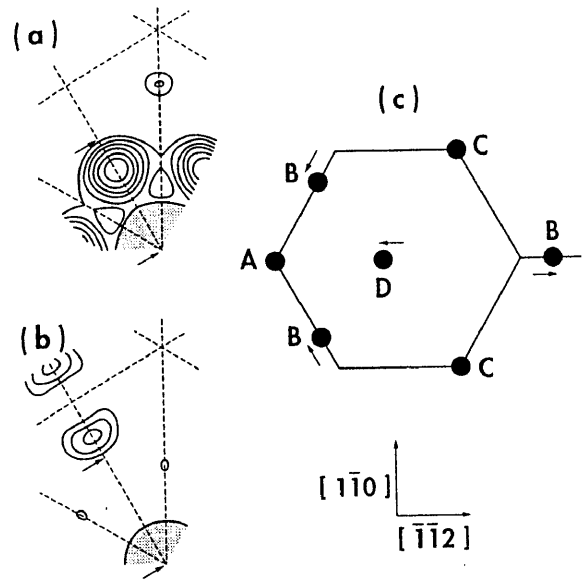


Figure 2. Partial Patterson maps for (a) boron and Si and for (b) Ge. Arrows indicate the unreconstructed in-plane bond length. From these maps the distorted hexagon in (c) is inferred.

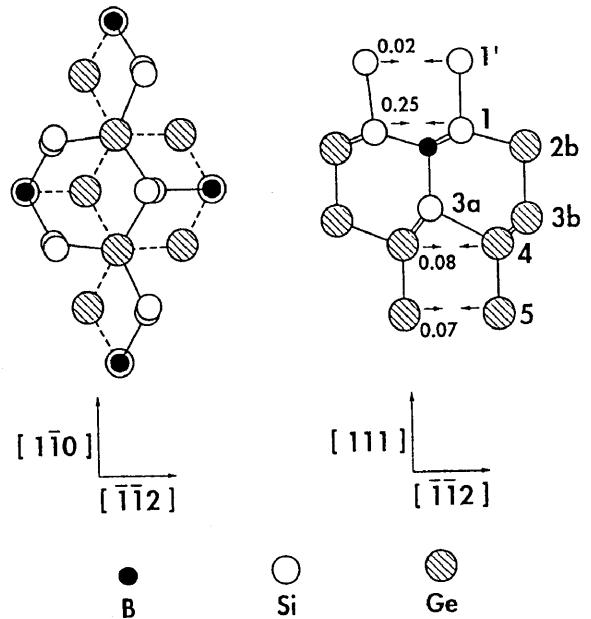
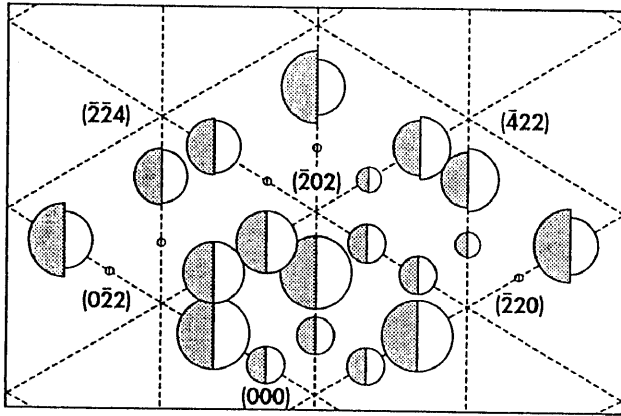


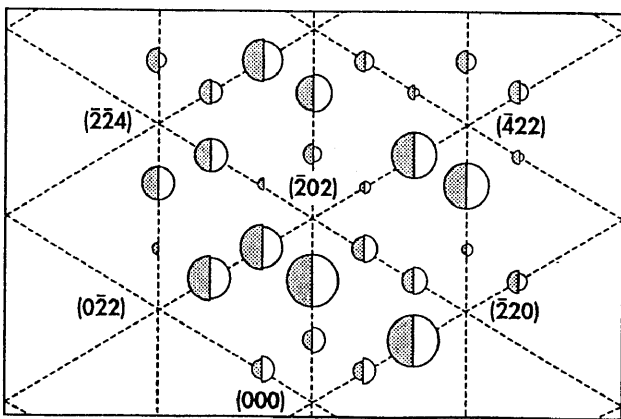
Figure 3. Model structure of the interface viewed from above (left) and from the side (right). In-plane distortions are indicated on units of angstroms.

taken from multiple measurements of equivalent reflections, but were set to at least 10%, typical of GID experiments. The difference in intensities between the left- and right-hand sides of the figure is due to a small component of the momentum transfer perpendicular to the interface. The overall fitting results is satisfying very well.

In conclusion, direct evidence for ordering of the Ge and Si atoms at this interface was obtained. Specially, it was found that boron lies in a substitutional site surrounded by four nearest-neighbor Si atoms with Ge in the other sites.



(a)



(b)

Figure 4. Maps of diffracted intensity from the reconstructed interface measured at X-ray energies of (a)  $E=8.266$  keV and (b)  $E=11.098$  keV. The dotted lines cross at the bulk fundamental lattice points, several of which are identified. The shaded left half circles show the measured intensities and the right half circles show the values calculated from the model structure of Fig. 3.

Due to the size considerations, one might expect that boron should be surrounded by Ge, not Si. However, binding-energy effects combined with a kinetic, surface-strain mechanism may explain this structure.

The improved thermal stability of  $B\sqrt{3}/Si(111)$  interfaces incorporating Ge has been also studied.<sup>7)</sup> The experiments were done using techniques with synchrotron radiation source to examine in-situ heterostructure growth by MBE. The details of the apparatus have been published elsewhere.<sup>8)</sup>

Figure 5 shows the results of the annealing experiments. The integrated peak intensities of each sample have been normalized to the value they had before the annealing process began. The B/Si sample starts to degrade sharply around 250°C while B/GeSi is stable to 350°C. In both, the reconstructed peak has become quite weak by the 600°C anneal. However, above this temperature the peak intensity of the B/Si sample recovers, becoming even stronger than at room temperature. RHEED shows a  $\sqrt{3}$  pattern, indicating that the a-Si has crystallized and the boron has migrated to

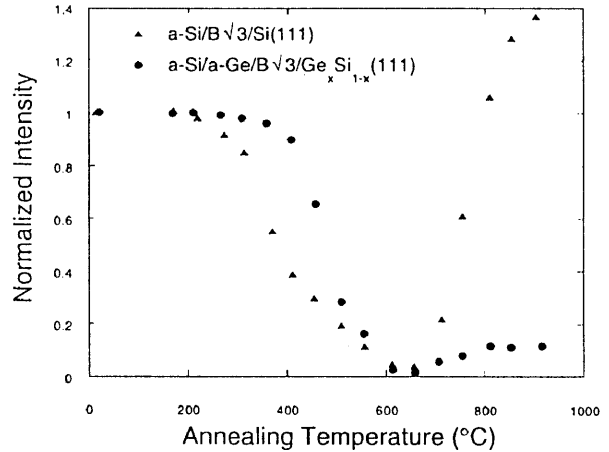


Figure 5. Results of the annealing experiment. Integrated X-ray intensities of a reconstructed peak versus annealing temperature. The intensities for both samples have been normalized to the value they had before the annealing process began. The measured peak was  $2/3(\bar{1}\bar{2}3)$ .

the surface, forming a  $\sqrt{3}$  reconstruction. In contrast, the intensity of the B/GeSi sample only slightly recovers above 600°C, suggesting that the boron atoms are still mostly trapped near the interface, although not in a  $\sqrt{3}$  structure. However, some must reach the surface, since RHEED shows a  $\sqrt{3}$  pattern for this sample as well. In conclusion, the thermal stability of  $B\sqrt{3}/Si(111)$  interfaces incorporating Ge has been improved. By Using the improved thermal stability at the GeSi interface, a heterostructure consisting of two  $B\sqrt{3}$  layers separated by a 40Å spacer has been successfully grown.<sup>7)</sup>

### 3. Interface Stress

For future LSI devices with high density memories, the necessary gate oxide thickness is estimated to be around 5-10 nm. For this thickness regime, a rapid decrease of the breakdown charge ( $Q_{bd}$ ) of  $SiO_2$  films has been observed in constant current time-dependent-dielectric-breakdown (TDDDB) measurements. The electronic properties of such thin films are affected by the structure of the  $SiO_2$  films. The existence of a structural transition layer at the  $SiO_2/Si$  interface has been reported by X-ray photoelectron spectroscopy experiments and studies of the etching speed of the  $SiO_2$  layer. Even a crystalline phase has been found at the  $SiO_2/Si$  interface by electron microscopy, and X-ray diffraction techniques.<sup>9)</sup> In spite of a number of structural studies of the  $SiO_2/Si$  interface, there are many remaining problems, such as the initial oxidation mechanism.

Recently, a grazing incidence X-ray diffraction geometry using synchrotron radiation has been widely used in structural studies of surfaces and interfaces. Those experiments were based on kinematical theory. However, when using bulk reflections of a nearly perfect crystal, such as Si or GaAs, dynamical effects must be taken into consideration. For the diffraction geometry of a small incident angle to the crystal surface and a large angle exiting from the surface, dynamical effects have been considered in detail by Kishino and Kohra.<sup>10)</sup> A few application works

were done in the field of surface-selective and interface-selective topography.

The X-ray intensity of the silicon substrate 311 reflection has been measured in an extremely asymmetric scheme of small incident angle and large exit angle for various silicon oxide thickness.<sup>11)</sup> Using the absorption of the SiO<sub>2</sub> films, it has been found that a low density (2.37-2.40 g/cm<sup>3</sup>) structural transition layer of silicon oxide exists for thin (7-8 nm) SiO<sub>2</sub> films on the silicon substrate, whereas the silicon oxide layer above 7-8 nm thick has the same density as bulk SiO<sub>2</sub> (2.55-2.60 g/cm<sup>3</sup>). The density is obtained from the slope of X-ray intensity versus SiO<sub>2</sub> thickness plots.<sup>11)</sup>

SiO<sub>2</sub> films were thermally grown on undoped (1000 Ωcm) floating-zone-grown (FZ) silicon (100) substrates to avoid the influence of oxygen-related bulk imperfections which appear in Czochralski-grown (CZ) substrates. Both surfaces of the substrate wafers were finished by mechanochemical polishing techniques to avoid backside damage which would otherwise give surface-side strain fields and also warp the wafer upon forming the SiO<sub>2</sub> films. All fabrication processes of the SiO<sub>2</sub> films were performed in ultraclean facilities, capable of producing state-of-the-art dynamic random access memories. The substrate wafers were chemically cleaned in (NH<sub>4</sub>OH+H<sub>2</sub>O<sub>2</sub>+H<sub>2</sub>O) and (HCl+H<sub>2</sub>O<sub>2</sub>+H<sub>2</sub>O) solutions. Next, the native oxide layer was removed by a dilute HF solution. The concentration of heavy metals and Na on the wafers was less than 5×10<sup>9</sup> atoms/cm<sup>2</sup>, as analyzed by vapor phase decomposition atomic adsorption spectrometry measurements. The SiO<sub>2</sub> films were fabricated in a usual resistance-heated quartz furnace under two different conditions: at a substrate temperature of 900°C in dry O<sub>2</sub> gas and at 750°C in a pyrogenic steam. The thickness of the SiO<sub>2</sub> films ranges

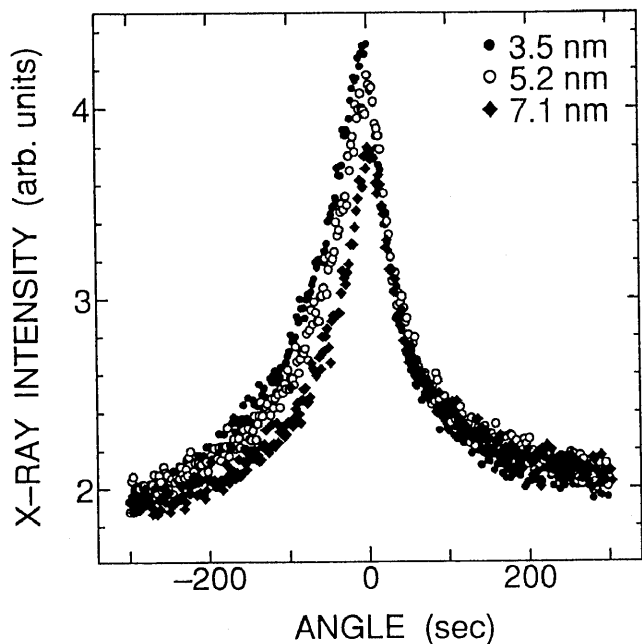


Figure 6. Representative rocking curves for three samples having different thickness SiO<sub>2</sub> films formed at 750°C in a pyrogenic steam. The X-ray intensities decrease with increasing film thickness due to absorption by the SiO<sub>2</sub> films. Curve profiles are not symmetric.

from 3.5 to 10.5 nm.

The X-ray intensity of the silicon substrate 311 reflection was measured in an extremely asymmetric scheme. By using successive 311 reflections from the monochromator crystals, the angular divergence of the X-rays impinging on the sample was less than 0.1 arcsec. The 311 reflection was used in a parallel setting to avoid wavelength-dispersion effects. The X-ray diffraction experiment was also performed at beam line 9C in the Photon Factory.

By tuning incident X-ray energy (about 1.40Å), the incident angle impinging on the sample crystal surface can be set near to the critical angle (about 0.2 degree) of total reflection.

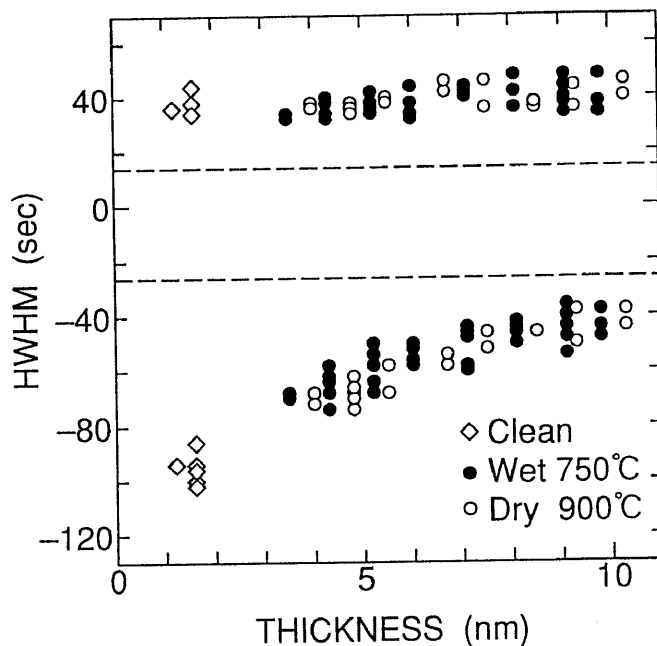


Figure 7. Half width at half maximum for the low angle side (negative values) and the high angle side (positive values) for various fabrication conditions. The expected HWHM values from theory<sup>10)</sup> are shown as dashed lines.

Representative X-ray intensity curves, which is measured in the  $\theta$ -scan (incident-angle scan), are shown in Fig. 6. In Fig. 6, curve profiles are not symmetric.

The half width of half maxima (HWHM) of X-ray rocking curves of the various fabrication condition are shown in Fig. 7. In Fig. 7, the fabrication process condition "clean" means silicon substrates with native oxide layer. The half width of half maxima of a low angle side of  $\theta$ -scan is drawn by negative value and that of a high angle side is drawn by positive value. Expected HWHM by the theory of Kishino and Kohra<sup>10)</sup> is shown as dashed line. It is found that in the thin SiO<sub>2</sub> region, the HWHM value of the low angle side is far from that expected by Kishino and Kohra.<sup>10)</sup> That is thought to be lattice expansion toward [311] direction.  $\Delta d / d$  is roughly estimated to be the order of 10<sup>-3</sup> ~ 10<sup>-4</sup>. This expansion can be controlled by surface treatment on initial Si surface before the formation of SiO<sub>2</sub> films.

In conclusion, X-ray rocking curve studies reveal that silicon substrate lattice is highly stressed even in the thin-SiO<sub>2</sub>/Si interface. This stress may be the reason for the existence of the degraded SiO<sub>2</sub> layer at the SiO<sub>2</sub>/Si interface through stress induced phenomenon.<sup>12)</sup>

- 1) K. Akimoto, I. Hirosawa, T. Tatsumi, H. Hirayama, J. Mizuki, and J. Matsui: *Appl. Phys. Lett.* **56** (1990) 1225.
- 2) D.J. Tweet, K. Akimoto, I. Hirosawa, T. Tatsumi, J. Mizuki, and J. Matsui: *Phys. Rev. Lett.* **69** (1992) 2236.
- 3) For a review, see J. Karle: *Physics Today* **42** (1989) 22.
- 4) K. Akimoto, K. Hirose, and J. Mizuki: *Phys. Rev.* **B44** (1991) 1622.
- 5) D.J. Tweet, and K. Akimoto: *Modern Phys. Lett.* **B8**, 721 (1994).
- 6) R.L. Headrick, I.K. Robinson, E. Vlieg, and L.C. Feldman: *Phys. Rev. Lett.* **63**, 1257 (1989).
- 7) D.J. Tweet, and K. Akimoto: *Physica B*, **221**, 218 (1996).
- 8) K. Akimoto, J. Mizuki, I. Hirosawa, and J. Matsui: *Rev. Sci. Instr.* **60**, 2362 (1989).
- 9) P. H. Fuoss, L. J. Norton, S. Brennan, and A. Fisher-Colbrie: *Phys. Rev. Lett.* **60**, 600 (1988).
- 10) S. Kishino and K. Kohra: *Jpn. J. Appl. Phys.* **10**, 551 (1971).
- 11) E. Hasegawa, A. Ishitani, K. Akimoto, M. Tsukiji, and N. Ohta: *J. Electrochemical Society*, **142** 273 (1995).
- 12) C. P. Flynn: *Phys. Rev. Lett.* **57**, 599 (1986).